coatings

Article

Improving the Surface Friction and Corrosion Resistance of Magnesium Alloy AZ31 by Ion Implantation and Ultrasonic Rolling

Zhongyu Dou *, Haili Jiang, Rongfei Ao, Tianye Luo and Dianxi Zhang

College of Physics and Electronic Science, Anshun University, Anshun 561000, China;
j200109012022@163.com (H.J.); arf1028@163.com (R.A.); rotiondemon@126.com (T.L.); xiwa_315@163.com (D.Z.)
* Correspondence: 2012620@asu.edu.com

Abstract: The use of the magnesium alloy AZ31 is common in aviation and biomedicine; however, this alloy has poor friction and corrosion resistance. Here, mechanical grinding, ultrasonic rolling, and ultrasonic rolling + ion implantation were performed on the magnesium alloy surface to study the effect of the treatment process on the friction and corrosion resistance of the magnesium alloy surface. The results show that the surface roughness of the magnesium alloy treated by ultrasonic rolling + ion injection is reduced more than mechanical grinding and ultrasonic rolling. The friction coefficient is the lowest, the wear resistance is the best, and new phase nitrogen compounds appear on the surface. The results of SBF (simulated body fluid) solution immersion showed that the sample treated via this composite process had the lowest corrosion rate, which was 62.45% and 58.47% lower than that of the mechanically ground samples. The surface was relatively intact after the corrosion test, and the corrosion resistance was the best. These results can provide a new strategy for magnesium alloy surface protection.

Keywords: magnesium alloy; ultrasonic rolling; ion implantation; friction and wear; corrosion

check for updates

Citation: Dou, Z.; Jiang, H.; Ao, R.; Luo, T.; Zhang, D. Improving the Surface Friction and Corrosion Resistance of Magnesium Alloy AZ31 by Ion Implantation and Ultrasonic Rolling. *Coatings* **2022**, *12*, 899. https://doi.org/10.3390/coatings12070899

Academic Editors: Matic Jovičević-Klug, Alina Vladescu, Patricia Jovičević Klug and László Tóth

Received: 26 May 2022
Accepted: 22 June 2022
Published: 25 June 2022

Publisher's Note: MDPI stays neutral with regard to jurisdictional claims in published maps and institutional affiliations.

Copyright: © 2022 by the authors. Licensee MDPI, Basel, Switzerland. This article is an open access article distributed under the terms and conditions of the Creative Commons Attribution (CC BY) license (https://creativecommons.org/licenses/by/4.0/).

1. Introduction

Magnesium alloys are a green and lightweight material and have a high specific strength, high specific stiffness, and low density. They can be used in new energy vehicles, biomedicine, aviation, and other fields [1,2], but their wear and corrosion resistance are severely restricted. Alloy composition deployment, alloy-processing technology, and alloy surface-coating technologies have all been proposed [3–7] and have enhanced the development of magnesium, its alloys, and alloy applications. However, these traditional protective-layer methods can only effectively protect the surface of the magnesium alloy when the protective layer exists. The magnesium alloy will still quickly corrode in a corrosive medium when the protective layer on the surface is damaged by corrosion. Thus, a protective coating is used. It is important to study whether the corrosion products are harmful to the body. The wear of ultra-high-molecular-weight polyethylene (UHMWPE) releases polyethylene wear particles, which can trigger a negative reaction of the body and promote osteolysis [8]. The biocompatibility of the protective layer needs to be considered.

Surface nanoscale treatment processes are a common and effective method. Researchers have performed different treatment processes such as surface mechanical grinding [9,10], shot peening [11,12], and laser treatment [13]. Although these have improved the mechanical properties, the surface quality of the material is reduced, which affects the friction and corrosion resistance. Liu et al. [14] found that the surface nanostructured layer of GW63K magnesium alloy after SMAT treatment had poor plasticity and toughness, thus resulting in worse wear resistance versus untreated alloys. Liu Mengen et al. [15] found that the corrosion resistance of high-energy shot peening on AZ31 magnesium alloy in 5% (mass fraction) NaCl solution is lower than that of untreated samples due to the formation of a large number of cracks on the surface during shot peening. As a result, the corrosion contact surface increases, thus resulting in a significantly higher corrosion rate of the shot-peened sample than the unpeened sample. The ultrasonic surface-rolling process (USRP) combines traditional rolling processes and ultrasonic technology to refine grains and improve performance. The surface quality of the workpiece is significantly improved [16]. Zhang Haiquan et al. [17] strengthened ZK60 magnesium alloys via a surface-rolling strengthening process. The results showed that rolling strengthening can significantly reduce the surface roughness of the material and introduce residual compressive stress to the surface of the material. Yang et al. [18] treated the magnesium alloy AZ31 via ultrasonic rolling and found that the surface grains of magnesium alloys were refined after rolling strengthening; the roughness was reduced and the friction properties were improved.

High-energy ion implantation technology (HEII) utilizes high-speed ion bombardment of pre-infiltrated elements from the target to achieve metallurgical bonding with the plated metal, thus improving the friction and corrosion resistance of the material. The material itself does not deform [19]. Lei et al. implanted Al ions into the surface of AZ31 magnesium alloy, and the friction and wear results showed that the wear rate of magnesium alloy was reduced by 30% [20]. Zhou et al. [21] used Zr to implant magnesium alloy ZK60 and found that the friction and corrosion resistance of magnesium alloy was effectively improved after implantation. Other studies [22,23] reported that N/Ti ion implantation improved the friction and corrosion resistance of magnesium alloy AZ31.

Dingshun [24] carried out USRP + PN (plasma nitriding) composite treatment on pure titanium TA2, and the infiltrated layer showed the best wear resistance and friction reduction performance. Dawen et al. [25] used USRP + HEII for composite treatment of 316 L. The surface hardness was increased by 57.8% versus single-HEII-treated samples; the thickness of the infiltration layer was nearly double that of a single-HEII-treated sample. In conclusion, ultrasonic rolling and ion implantation are effective means of improving the surface properties of magnesium alloys. Surprisingly, the influence of the composite treatment technology on the properties of the magnesium alloys is rarely reported.

Therefore, the effects of mechanical grinding, ultrasonic rolling, and USRP + HEII on the surface structure, friction resistance, and corrosion resistance of magnesium alloys are reported in this study. The results offer a reference for the development of treatment technologies for magnesium alloy surface protection.

2. Materials and Methods

2.1. Material and Sample Preparation

The test material was rolled AZ31 magnesium alloy purchased from a domestic factory; the chemical composition is shown in Table 1. Magnesium alloy sheets were rolled and strengthened using ultrasonic-rolling equipment (customized). The size was $15 \times 15 \times 5$ mm as cut by a wire electric discharge machine. High-energy N ion implantation was performed using ion implantation equipment (Southwestern Institute of Physics, Chengdu, China). The magnesium alloy was polished with 1000# and 2000# water-grinding sandpaper and then polished; this sample was marked as S1. The sample after ultrasonic rolling was designated as S2. The static pressure was 0.15 MPa, the feed speed was 4000 mm/min, and the rolling treatment was 1 pass. The ion implantation sample after rolling was marked as S3. It had an implantation energy of 40 keV. The implantation dose was 1×10^{18} icons/cm^2 and the vacuum was 3.9×10^{-3} Pa.

Table 1. Chemical composition of AZ31 magnesium alloy (wt%).

Al	Zn	Mn	Si	Ca	Cu	Fe	Ni	Mg
2.5–3.5	0.6–1.4	0.2–1.0	0.08	0.04	0.04	0.003	0.001	Remainder

2.2. Microstructure and Performance Characterization

Magnesium alloy samples with different treatments were analyzed with an X-ray diffractometer (PANalytical X Pert PRO, Almelo, Holland). The detection angle was 20–80°, the speed was 2°/min, and the step size was 0.013/s. The three-dimensional topography and surface roughness of the treated magnesium alloy surfaces were measured by atomic force microscopy (Bruker Dimension Icon AFM, Karlsruhe, Germany). The surface mechanical and friction properties were investigated using a microhardness tester (HMV-G, Kyoto, Japan) and a friction and wear-testing machine (Bruker UMT-2, Karlsruhe, Germany). A Phase Shift MicroXAM-3D (MicroXAM-3D, Milpitas, USA) measured the wear volume of the samples after wear to judge the extent of wear. The hardness test selected five points to obtain the average value. The load was 0.98 N and the duration was 10 s. The room-temperature dry-friction test was performed with 10 mm Al_2O_3 balls (HRC95). The circumferential speed was 100 rpm/min, the load was 10 N, and the duration was 20 min. The wear-scar radius was 12 mm.

The AZ31 magnesium alloy samples were ultrasonically cleaned in ethanol before soaking, and then dried in cold air. The samples with different treatments were encapsulated with oxidized resin with an exposed area of 1 cm^2. They were then weighed with an electronic balance. The encapsulated samples were soaked in SBF at 37 ± 0.5 °C for 48 h, and 55% of the solution was renewed every 24 h to simulate natural human body-fluid renewal. The sample was soaked in a 5% NaCl solution for 72 h. Specimens were cleaned according to ASTM Standard G31-72 and then weighed. Each sample was placed in concentrated nitric acid for 5 min to remove corrosive products. The degradation performance of the samples under different treatment processes in SBF (simulated body fluid) and NaCl solution was evaluated via the weight-loss method. The corrosion rate **V** was calculated by the weight-loss method (G31-72 standard) using the following formula [26]: $v = (K \times \Delta m)/(A \times t)$, where K is the constant pole, Δm is the mass loss of the sample before and after soaking, A is the exposed area of the sample, and t is the soaking time. Scanning electron microscopy (VEGA3, Brno, Czech Republic) was used to observe the surface morphology of the magnesium alloy samples after immersion to remove corrosive products. Before observing the corrosion morphology, anhydrous ethanol was used for ultrasonic cleaning for 5 min and dried with cold air.

3. Results

3.1. Phase Analysis

Figure 1 shows XRD patterns of the AZ31 magnesium alloys treated under different processes. The XRD peaks of the compounds were found by comparing PDF cards (#35-0821, #45-0946, #01-1289). No new diffraction peaks appeared in the XRD patterns after ultrasonic-rolling treatment versus untreated samples. The untreated samples and the ultrasonic-rolling test show only Mg phases and MgO phases in the samples, thus indicating that the ultrasonic-rolling process did not lead to the formation of new phases in the samples. There were no obvious changes in the diffraction spectrum due to the low content of $Mg_{17}Al_{12}$ phase in the original material [27]. The XRD pattern of the ultrasonic-rolling sample after ion implantation had Mg phases and MgO phases. There was also an Mg_3N_2 phase formed after N ion implantation, thus indicating that the ions and the inherent elements in the matrix would combine with each other during the implantation process to form a new phase. The diffraction peak position and intensity of the surface phase of the sample changed before and after implantation due to the deformation of the surface-lattice structure caused by the internal stress generated upon bombardment of the ion implantation. Holes formed on the surface and generated dislocations and many defects. The formation of an amorphous structure affected the preferred orientation of the same phase in the grains, thus resulting in changes in the position and intensity of its diffraction peaks.

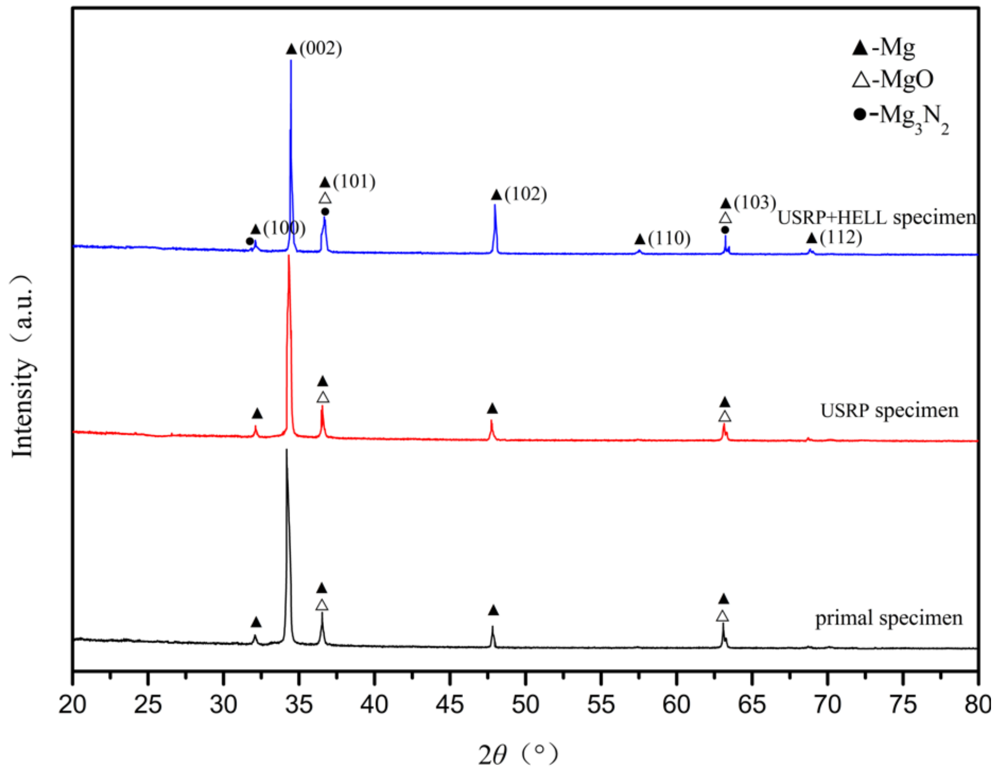

Figure 1. XRD patterns of magnesium alloy samples treated by different processes.

3.2. Surface Roughness and Microhardness

Surface roughness is an important indicator to measure the surface quality of materials and is an important factor affecting the performance of its mechanical parts. Figure 2 shows the three-dimensional surface morphologies of the magnesium alloy samples after different treatments. Surface roughness and microhardness information is shown in Table 2. The roughness of the AZ31 magnesium alloy after ultrasonic rolling was greatly reduced, and the surface quality was greatly improved. The surface quality of the magnesium alloy after ion implantation was further improved, and the average roughness value was reduced by 60% compared to the polished AZ31 magnesium alloy. The surface hardness increased by 23% after ultrasonic-rolling treatment, and the surface hardness was further improved after composite processing.

Table 2. Roughness and microhardness information.

Sample (#)	Primal Specimen	USRP Specimen	USRP + HELL Specimen
RMS roughness (nm)	87.4	42.7	35.0
Average roughness (nm)	64.2	34.3	26.0
Microhardness (HV)	60.2	73.3	81.6

Plastic flow occurred on the surface of the USRP specimen under the action of multi-directional force during ultrasonic rolling; thus, the “peaks” on the material surface flowed into the “valleys,” significantly reducing the mechanical defects (scratches) of the original specimen. The addition of lubricating oil on the surface of the sample further reduced the friction between the ball of the processing head and the surface of the sample, and thus the ultrasonic surface-rolling treatment significantly reduced the surface roughness of the sample [28]. Further reduction of surface roughness after ion implantation may have been due to sputtering, etching, and diffusion processes under this implantation dose. The results of the microhardness showed an increase in microhardness and the formation of a hardened layer after ultrasonic surface-rolling treatment. These results are due to the fact that ultrasonic-rolling treatment can produce better deformation hardening effects and fineness in the surface layer within a certain depth of the material. The grain-strengthening effect is caused by grain refinement, strain strengthening, and residual compressive stress. Studies have shown [29,30] that a smaller grain leads to greater microhardness. Hard phases such as Mg_3N_2 in the modified layer after N ion implantation are the main reasons for the increased microhardness.

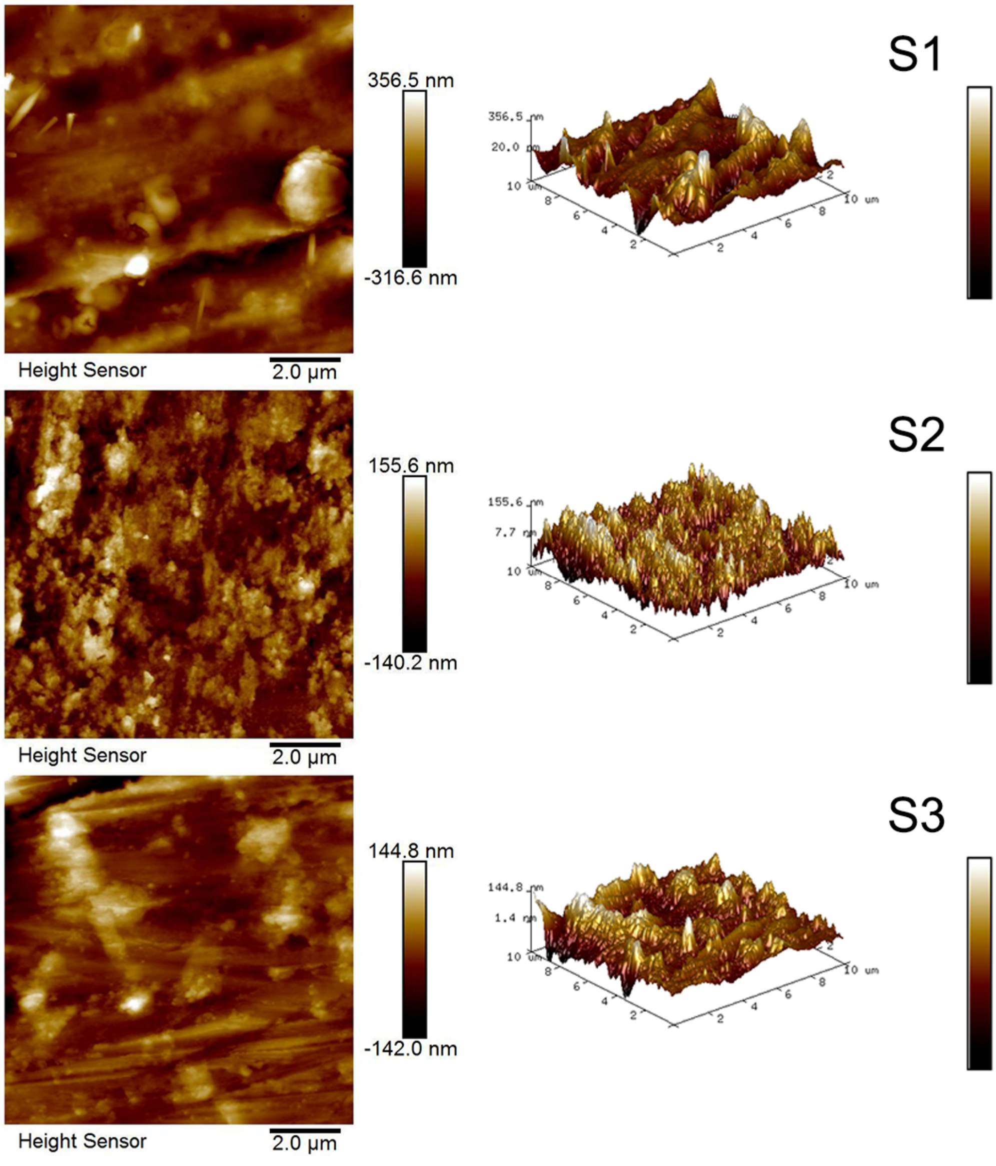

Figure 2. Three−dimensional AFM images of the samples: (**S1**) primal specimen, (**S2**) USRP specimen, (**S3**) USRP + HELL specimen.

3.3. Friction and Wear Performance

The coefficient of friction is the ratio of the frictional force between two surfaces to the vertical force acting on one surface. A smaller coefficient of friction leads to more wear resistance. The coefficient of friction is related to such factors as the surface roughness, hardness, and strength. The friction coefficient curves of AZ31 magnesium alloy samples treated with different processes are shown in Figure 3: At the beginning of friction, the friction coefficient of magnesium alloy samples treated with different processes increased with almost the same slope and then fluctuated within a certain interval. In the initial running-in wear stage, the softer substrate was first worn away by the harder surface of the friction pair, thus resulting in furrows, fractures, or chips; the friction factor was larger. The friction coefficient then stabilized. The average friction coefficient of the original AZ31 magnesium alloy was about 0.321 in the 1200 s test period. The friction coefficient of the samples in the ultrasonic rolling place were improved due to the improved surface quality. The average friction coefficient was about 0.29, and the friction coefficient of the USRP specimen was smaller than the ground specimen throughout the entire friction process. The friction coefficient of the samples after N ion implantation was further reduced, and the average friction coefficient was about 0.276 due to the combined effect of the emergence of hardened phase nitrides, hardness enhancement, and surface roughness after ion implantation.

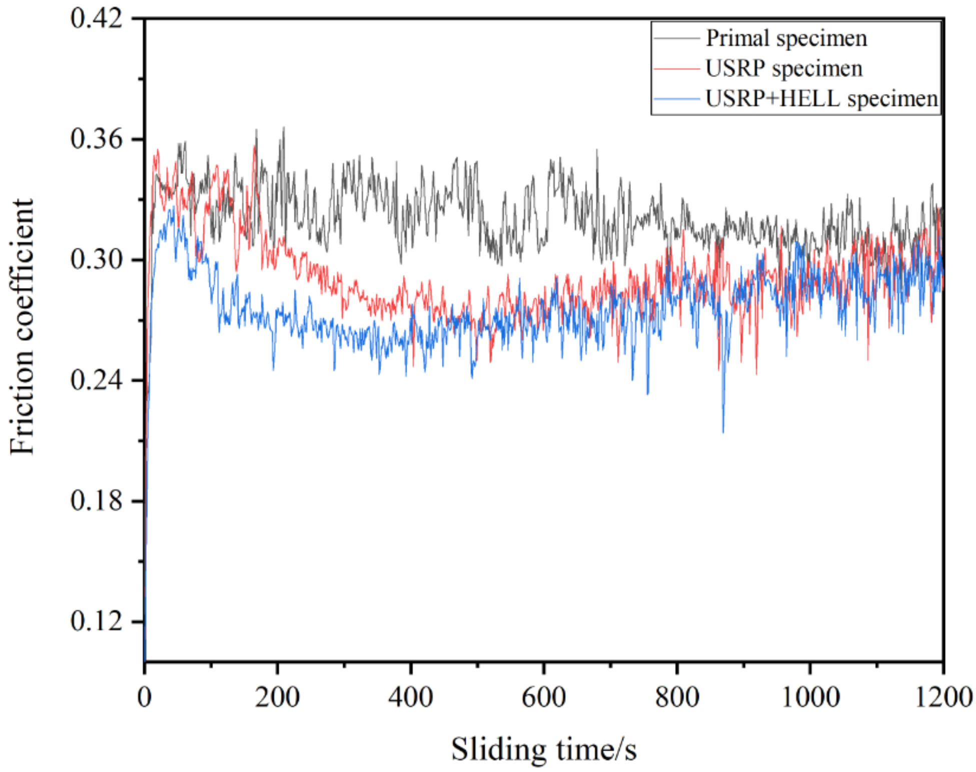

Figure 3. Variation curve of the friction coefficient of different samples.

The amount of wear directly reflects the wear resistance of the material. Thickness, mass, and volume are three ways to characterize the wear amount. The wear resistance was evaluated by measuring the volume wear of the samples treated with different processes. The volume wear of the samples with the three treatments is shown in Figure 4. The figure shows that the volume wear of the samples treated by ultrasonic rolling was significantly smaller than the original magnesium alloy under the same experimental conditions. The volume wear of the composite-treated samples was the smallest and was related to the friction coefficient. The performance was consistent, thus indicating that the ultrasonic-rolling process can significantly improve the wear resistance of magnesium alloy materials. The wear resistance of the materials treated by the USRP + HELL composite process was further improved, which proves that ion-implantation technology based on prefabricated nanostructured layers is an effective method to improve the friction and wear properties of magnesium alloys. Figure 5 shows the SEM morphology of the wear track. The morphology of sample S1 showed obvious grooves and pits, the plastic deformation was serious, and a large amount of wear-scar debris appeared on the surface of the wear scar, indicating that the polished magnesium alloy sample had adhesive wear and abrasive particles, which is the main wear mechanism of magnesium alloys. Compared with sample S1, the furrows caused by micro-cutting in the rolled samples were still more obvious, but the grooves were shallow and narrow, the plastic deformation was reduced, and the abrasive wear condition was improved. The surface of the sample S3 treated by the composite process was relatively flat, the plastic deformation was greatly improved, the adhesion of debris was greatly improved compared to the former two, and the wear debris was granular. The shape of the wear debris was proportional to the degree of wear [31], indicating that the load-bearing capacity of the specimen was improved after the composite treatment process, which is consistent with the performance of the irradiation strengthening study [32], and the results of the wear volume loss also illustrate this point. The improvement in friction and wear performance was due to the substantial reduction of surface roughness and the increased surface hardness; it may also be that high residual compressive stress was introduced into the surface layer, forming a gradient nanostructure that inhibited the initiation and expansion of microcracks in the surface layer and improved the friction and wear properties of the material.

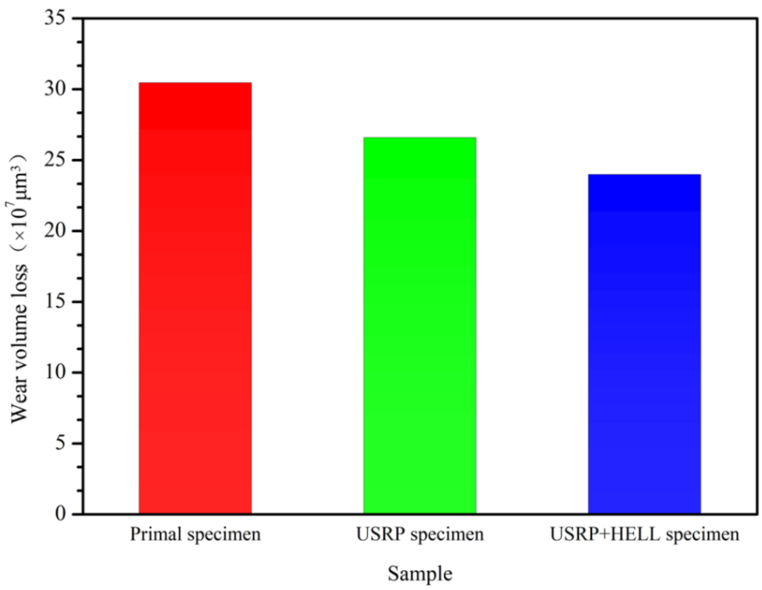

Figure 4. Wear volume loss of samples with different treatment processes.

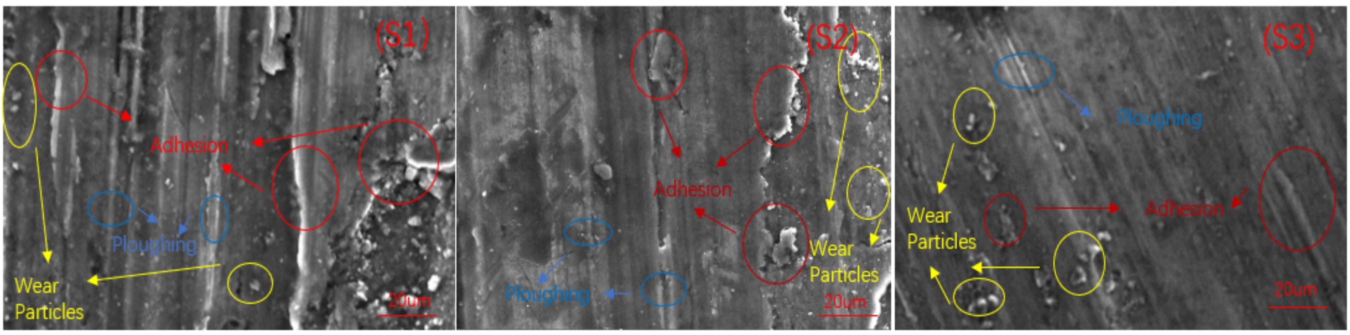

Figure 5. SEM images of worn morphologies of the (**S1**) primal sample; (**S2**) USRP sample; (**S3**) USRP + HELL sample.

3.4. Corrosion Performance

The corrosion morphology of the sample in Figure 6 shows that the surface of sample S1 (Figure 6a) had a large and deep corrosion area after corrosion in the SBF solution; there were corrosion impurities after the corrosion reaction. The residue covered most of the surface with obvious corrosion pits. The report by [33] pointed out that the corrosion of AZ31 after immersion in SBF solution appeared as voids, and the corrosion products included $MgO/Mg(OH)_2$ and $Ca_{10}(PO_4)_6(OH)_2$ phases. The corrosion pits of sample S2 (Figure 6b) were much smaller, and most of them were pitting pits. The surface of sample S3 (Figure 6c) was corroded in a semi-uniform way. The fine corrosion cracks were distributed along the grain boundaries in a network shape. After the immersion test in NaCl solution, the corrosion products were dominated by $Mg(OH)_2$ phase [34,35]. It can be seen that the corrosion conditions were greatly improved after different treatments (versus Figure 6c,d), and the surface of the sample treated via the composite process was much smoother than sample (S1) in terms of corrosion resistance.

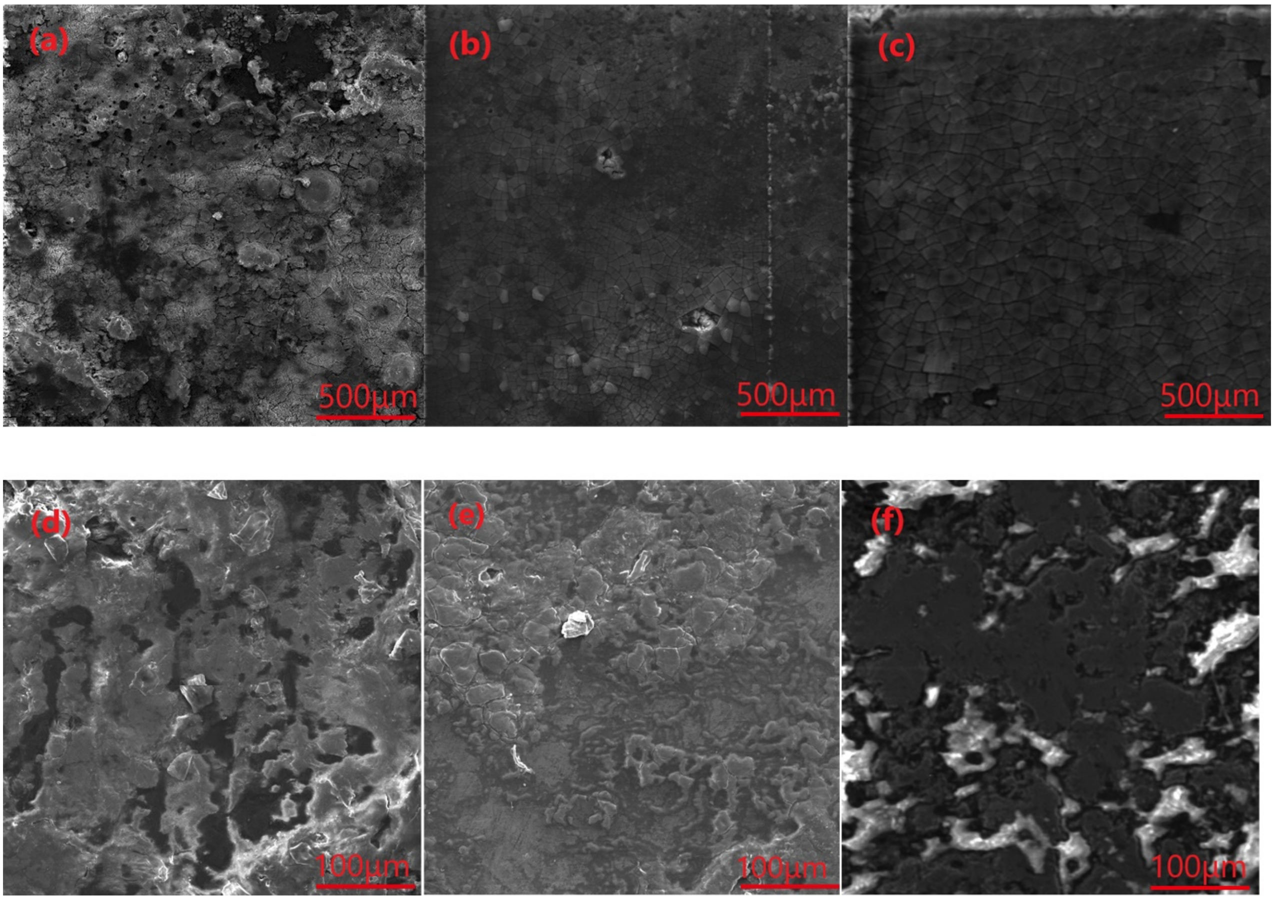

Figure 6. Typical SEM images of samples with different treatments immersed in SBF solution and 5 wt% NaCl aqueous solution: (**a**,**d**) primal sample; (**b**,**e**) USRP sample; (**c**,**f**) USRP + HELL sample.

Figure 7 shows the corrosion information of the magnesium alloy samples obtained after the immersion experiment. The performance was relatively consistent in the two corrosion solutions. Ref. [33] pointed out that magnesium alloy AZ31 had the highest degradation rate of Mg in SBF solution compared with other solutions, which is also the reason why AZ31 magnesium alloy degrades the fastest in SBF solution. The ultrasonic-rolling treatment reduced the corrosion rate of the surface of the magnesium alloy sample due to the ultrasonic-rolling process. The surface of the magnesium alloy then formed a high-density plastic deformation layer. The crystal size was refined versus the original magnesium alloy sample, and the grain boundary was significantly increased. Many grain boundaries blocked the continuous erosion of the sample and prevented the development trend of tiny cracks and the widening of the etched holes in the substrate [36]. Refs. [37–39] pointed out that the surface roughness and grain size of the alloy significantly affect the corrosion resistance, and the nanostructured surface grains enhance the formation of the surface passivation layer, thereby improving the corrosion resistance of the material. Therefore, the surface roughness and grain refinement of the samples after ultrasonic rolling improved the corrosion resistance of the samples. The ion-implantation process after ultrasonic rolling further delayed the corrosion reaction on the surface of the sample, and the degradation rates of the samples in SBF and NaCl solutions were 62.45% and 58.47% lower, respectively, than those of the mechanically ground samples. In addition to grain refinement and compressive stress after ultrasonic rolling, N ions, as an interstitial element, formed an interstitial solid solution after implantation, which made it easy to form an amorphous surface and improve the resistance to pitting corrosion. After ionization and acceleration of ion implantation, high-energy ions were implanted into the surface of the workpiece, and a series of collisions occurred with atoms and electrons near the surface, generating strong energy and resulting in changes in the structure and organization of the effective processing layer. The modified layer was composed of the compounds MgO and Mg_3N_2 with very good corrosion resistance. When the implantation dose reached a certain critical value, the implanted layer became disordered, and the structure had good anti-oxidation and anti-corrosion ability [40,41]. The residual pressure increased the strength of the $Mg(OH)_2$ protective film due to the large residual stress generated after rolling and ion implantation; thus, it improved the corrosion resistance [42].

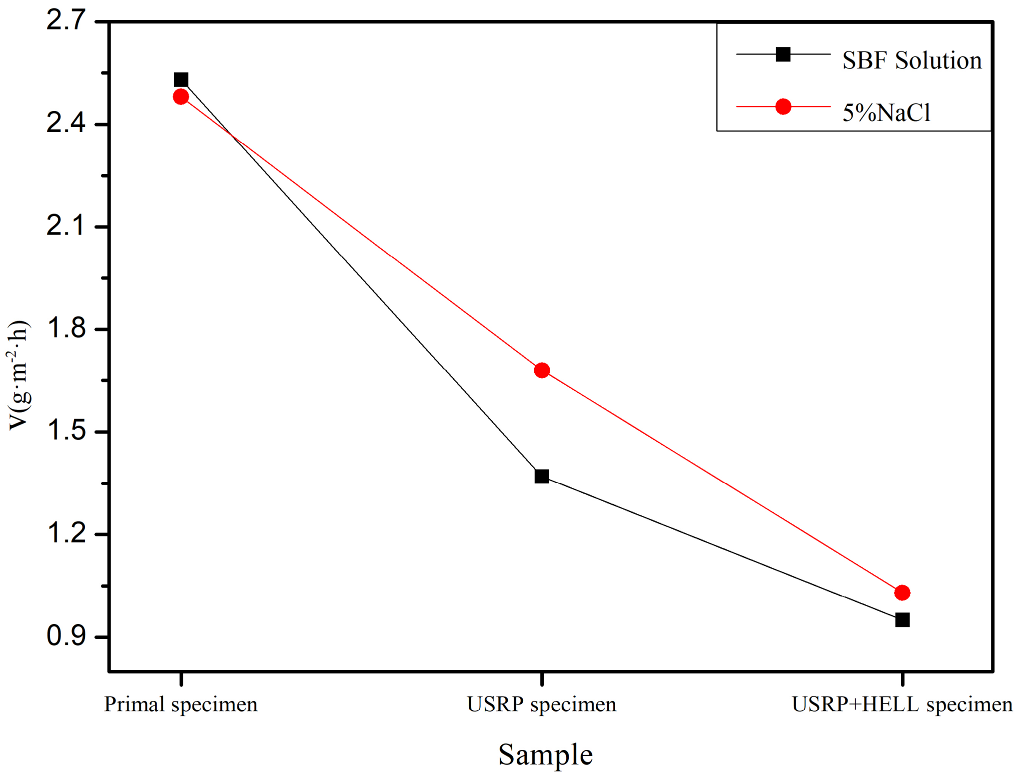

Figure 7. Corrosion information of magnesium alloy specimens after immersion experiments in two solutions.

In summary, the comprehensive effects of surface roughness, grain refinement, and residual compressive stress after USRP + HELL composite process further improved the corrosion resistance of magnesium alloy surfaces, thus indicating that the USRP + HELL composite is the best way to improve the friction and corrosion resistance of magnesium alloys. This is an effective method, and it is worth further studying the effect of composite treatment process parameters on the microstructure and properties of magnesium alloys.

4. Conclusions

In this study, magnesium alloys were processed via different treatment processes. The results showed that compared with mechanical grinding and ultrasonic rolling, the magnesium alloy treated by the USRP + HELL composite process had the lowest surface roughness, the highest hardness, the lowest friction coefficient, and the best wear resistance, and the adhesion wear on the surface was greatly improved. The reason for the improved friction and wear performance was due to the combined effect of the appearance of the hardened phase nitride after ion implantation, the surface roughness, and the residual compressive stress. The immersion experiment showed that the USRP treatment process could improve its corrosion resistance, but the corrosion rate was further reduced after the composite treatment process, which was 62.45% and 58.47% lower than that of the mechanically ground samples, and the larger residual stress further improved the corrosion resistance of magnesium alloys. The effects of three different treatment processes on the wear resistance and corrosion resistance of magnesium alloys are discussed, but the effects of USRP process and ion implantation process parameters on the microstructure and properties of magnesium alloys are not discussed. The effects of USRP + HELL process parameters on the surface structure and friction and corrosion resistance of magnesium alloys need to be further studied, and the research results can provide new references and ideas for surface-protection technology.

Author Contributions: Conceptualization, Z.D. and D.Z.; methodology, H.J.; software, H.J.; validation, Z.D., R.A. and T.L.; formal analysis, R.A.; investigation, H.J., R.A. and T.L.; resources, Z.D.; data curation, Z.D.; writing—original draft preparation, Z.D.; writing—review and editing, D.Z.; visualization, D.Z.; project administration, Z.D.; funding acquisition, Z.D. All authors have read and agreed to the published version of the manuscript.

Funding: This research was funded by the Youth Growth Project of The Education Department of Guizhou Province (2022040), the Key Laboratory of Materials Simulation and Computing of Anshun University (Asxyxkpt201803), the Key Supporting Discipline of Materials and Aviation of Anshun College (2020), and the National Undergraduate Innovation and Entrepreneurship Training Program of China (202110667005).

Institutional Review Board Statement: Not applicable.

Informed Consent Statement: Not applicable.

Data Availability Statement: No new data were created or analyzed in this study. Data sharing is not applicable to this article.

Acknowledgments: The author would like to give thanks for the equipment and technical support provided by Mechanical and Electrical Research and Design Institute of Guizhou Province, the Youth Growth Project of The Education Department of Guizhou Province (2022040), the Key Laboratory of Materials Simulation and Computing of Anshun University (Asxyxkpt201803), the Key Supporting Discipline of Materials and Aviation of Anshun College (2020), and the National Undergraduate Innovation and Entrepreneurship Training Program of China (202110667005).

Conflicts of Interest: The authors declare no conflict of interest.

References

1. Esmaily, M.; Svensson, J.E.; Fajardo, S.; Birbilis, N.; Frankel, G.S.; Virtanen, S.; Arrabal, R.; Thomas, S.; Johansson, L.G. Fundamentals and advances in magnesium alloy corrosion. *Prog. Mater. Sci.* **2017**, *89*, 92–193. [CrossRef]
2. Ding, W.; Wu, Y.; Peng, L.; Zeng, X.; Lin, D.; Chen, B. Research and application development of advanced magnesium alloys. *Mater. China* **2010**, *29*, 37–45.
3. Ma, R.; Lv, S.; Xie, Z.; Yang, Q.; Yan, Z.; Meng, F.; Qiu, X. Achieving high strength-ductility in a wrought Mg–9Gd–3Y–0.5Zr alloy by modifying with minor La addition. *J. Alloy. Compd.* **2021**, *884*, 1–12. [CrossRef]
4. Jana, A.; Das, M.; Balla, V.K. Effect of heat treatment on microstructure, mechanical, corrosion and biocompatibility of Mg-Zn-Zr-Gd-Nd alloy. *J. Alloy. Compd.* **2020**, *821*, 153462. [CrossRef]
5. Chen, B.; Wang, D.; Zhang, L.; Geng, G.; Yan, Z.; Eckert, J. Correlation between the crystallized structure of Mg67Zn28Ca5 amorphous alloy and the corrosion behavior in simulated body fluid. *J. Non-Cryst. Solids* **2020**, *553*, 120473. [CrossRef]
6. Zaludin, M.A.F.; Jamal, Z.A.Z.; Derman, M.N.; Kasmuin, M.Z. Fabrication of calcium phosphate coating on pure magnesium substrate via simple chemical conversion coating: Surface properties and corrosion performance evaluations. *J. Mater. Res. Technol.* **2019**, *8*, 981–987. [CrossRef]
7. Zhou, Z.; Zheng, B.; Lang, H.; Qin, A.; Ou, J. Corrosion resistance and biocompatibility of polydopamine/hyaluronic acid composite coating on AZ31 magnesium alloy. *Surf. Interfaces* **2020**, *20*, 100560. [CrossRef]

8. Jamari, J.; Ammarullah, M.I.; Santoso, G.; Sugiharto, S.; Supriyono, T.; Prakoso, A.T.; Basri, H.; van der Heide, E. Computational contact pressure prediction of CoCrMo, SS 316L and Ti6Al4V femoral head against UHMWPE acetabular cup under gait cycle. *J. Funct. Biomater.* **2022**, *13*, 64. [CrossRef]
9. Tao, N.R.; Wang, Z.B.; Tong, W.P.; Sui, M.L.; Lu, J.; Lu, K. An investigation of surface nanocrystallization mechanism in Fe induced by surface mechanical attrition treatment. *Acta Mater.* **2002**, *50*, 4603–4616. [CrossRef]
10. Xia, S.; Liu, Y.; Fu, D.; Jin, B.; Lu, J. Effect of surface mechanical attrition treatment on tribological behavior of the AZ31 alloy. *J. Mater. Sci. Technol.* **2016**, *32*, 1245–1252. [CrossRef]
11. Wu, S.X.; Wang, S.R.; Wang, G.Q.; Yu, X.C.; Liu, W.T.; Chang, Z.Q.; Wen, D.S. Microstructure, mechanical and corrosion properties of magnesium alloy bone plate treated by high-energy shot peening. *Trans. Nonferrous Met. Soc. China* **2019**, *29*, 1641–1652. [CrossRef]
12. Liu, H.; Jiang, C.; Chen, M.; Wang, L.; Ji, V. Surface layer microstructures and wear properties modifications of Mg-8Gd-3Y alloy treated by shot peening. *Mater. Charact.* **2019**, *158*, 109952. [CrossRef]
13. Guo, Y.; Wang, S.; Liu, W.; Sun, Z.; Zhu, G.; Xiao, T. Effect of laser shock peening on tribological properties of magnesium alloy ZK60. *Tribol. Int.* **2020**, *144*, 106138. [CrossRef]
14. Liu, Y.; Jin, B.; Li, D.J.; Zeng, X.Q.; Lu, J. Wear behavior of nanocrystalline structured magnesium alloy induced by surface mechanical attrition treatment. *Surf. Coat. Technol.* **2015**, *261*, 219–226. [CrossRef]
15. Liu, M.E.; Sheng, G.M.; Yin, L.J. Effects of high energy shot peening for magnesium alloy AZ31 on the corrosion properties and microhardness. *Funct. Mater.* **2012**, *43*, 2702–2704.
16. Fei, Z.; Xuchao, S.G. Effect of Surface Ultrasonic Rolling Treatment on Fatigue Properties of AISI304 Stainless Steel. *Chin. J. Hot. Manuf. Technol.* **2017**, *46*, 136–140.
17. Haiquan, Z.; Peiquan, G. Experimental Research on Surface Rolling Strengthening of ZK60 Magnesium Alloy. *Chin. J. Manuf. Technol. Mach. Tool* **2020**, *02*, 93–97.
18. Xilian, Y.; Yu, Z.; Wenting, H.; Meihong, H. Effect of ultrasonic surface rolling on friction and wear properties of AZ31B magnesium alloy. *Spec. Cast. Non-Ferr. Alloy.* **2020**, *40*, 1214–1218.
19. Yangyang, T.; Linbo, L.; Chao, W.; Zhao, F.; Weibo, M. Research Status of Ultrasonic Surface Rolling Nanotechnology. *Chin. J. Surf. Technol.* **2021**, *50*, 160–169.
20. Lei, M.K.; Li, P.; Yang, H.G.; Zhu, X.M. Wear and corrosion resistance of Al ion implanted AZ31 magnesium alloy. *Surf. Coat. Technol.* **2007**, *201*, 5182–5185. [CrossRef]
21. Ba, Z.; Jia, Y.; Dong, Q.; Li, Z.; Kuang, J. Effect of Zr ion implantation on wear and corrosion resistance of magnesium alloy. *J. Mater. Heat Treat.* **2019**, *40*, 135–142.
22. Fei, C.; Hai, Z.; Suo, C.; Fanxiu, L.; Chengming, L. Corrosion resistance properties of AZ31 magnesium alloy after Ti ion implantation. *Rare Met.* **2007**, *26*, 142–146.
23. Liu, H.; Xu, Q.; Jiang, Y.; Wang, C.; Zhang, X. Corrosion resistance and mechanical property of AZ31 magnesium alloy by N/Ti duplex ion implantation. *Surf. Coat. Technol.* **2013**, *228* (Suppl. 1), S538–S543. [CrossRef]
24. WenHua, X.; ShouZhou, W. Effect of surface nanocrystallization pretreatment on tribological properties of nitrogen layers of 316L stainless steel. *Mater. Prot.* **2017**, *50*, 23–27.
25. Zhao, X.H.; Nie, D.W.; Xu, D.S.; Liu, Y.; Hu, C.H. Effect of gradient nanostructures on tribological properties of 316L stainless steel with high energy ion implantation tungsten carbide. *Tribol. Trans.* **2019**, *62*, 189–197. [CrossRef]
26. ASTM G31-72. Standard Practice for Laboratory Immersion Corrosion Testing of Metals. ASTM: West Conshohocken, PA, USA, 1990.
27. Jialong, Z.; Liwei, L.; Wei, K.; Bo, C.; Minhao, L.; Yutian, F.; Min, M. Effect of cryogenic treatment on microstructure and mechanical properties of AZ31 magnesium alloy Sheet after Rolling. *J. Plast. Eng.* **2010**, *29*, 126–133.
28. Zhao, X.H.; Liu, K.C.; Xu, D.S.; Liu, Y.; Hu, C.H. Effects of ultrasonic surface rolling processing and subsequent recovery treatment on the wear resistance of AZ91D Mg alloy. *Materials* **2020**, *13*, 5705. [CrossRef]
29. Yu, H.; Xin, Y.; Wang, M.; Liu, Q. Hall-petch relationship in Mg alloys: A review. *J. Mater. Sci. Technol.* **2018**, *34*, 248–256. [CrossRef]
30. Andani, M.T.; Lakshmanan, A.; Sundararaghavan, V.; Allison, J.; Misra, A. Quantitative study of the effect of grain boundary parameters on the slip system level Hall-Petch slope for basal slip system in Mg-4Al. *Acta Mater.* **2020**, *200*, 148–161. [CrossRef]
31. Ye, H.; Sun, X.; Liu, Y.; Rao, X.; Gu, Q. Effect of ultrasonic surface rolling process on mechanical properties and corrosion resistance of AZ31B Mg alloy. *Surf. Coat. Technol.* **2019**, *372*, 288–298. [CrossRef]
32. Li, P.; Han, X.G.; Xin, J.P.; Zhu, X.P.; Lei, M.K. Wear and corrosion resistance of AZ31 magnesium alloy irradiated by high-intensity pulsed ion beam. *Nucl. Instrum. Methods Phys. Res.* **2008**, *266*, 3945–3952. [CrossRef]
33. Mena-Morcillo, E.; Veleva, L. Degradation of AZ31 and AZ91 magnesium alloys in different physiological media: Effect of surface layer stability on electrochemical behaviour. *J. Magnes. Alloy.* **2020**, *8*, 667–675. [CrossRef]
34. Wang, L.; Shinohara, T.; Zhang, B. Corrosion behavior of Mg, AZ31, and AZ91 alloys in dilute NaCl solutions. *J. Solid State Electrochem.* **2010**, *14*, 1897–1907. [CrossRef]
35. Xin, R.; Li, B.; Li, L.; Liu, Q. Influence of texture on corrosion rate of AZ31 Mg alloy in 3.5 wt.% NaCl. *Mater. Des.* **2011**, *32*, 4548–4552. [CrossRef]

36. Jinzhong, L.; Shijie, J.; Liujun, W.; Kaiyu, L. Effect of Laser Shock-Ultrasonic Rolling Composite Process on Mechanical Properties of AZ91D Magnesium Alloy. *Chin. J. Jilin Univ. Eng. Technol. Ed.* **2020**, *50*, 1301–1309.
37. Li, Y.; Zhang, T.; Wang, F.H. Effect of micro crystallization on corrosion resistance of AZ91D alloy. *Electrochim. Acta* **2006**, *51*, 2845. [CrossRef]
38. Pandey, V.; Singh, J.K.; Chattopadhyay, K.; Srinivas, N.C.S.; Singh, V. Influence of ultrasonic shot peening on corrosion behavior of 7075 aluminum alloy. *J. Alloy. Compd.* **2017**, *723*, 826–840. [CrossRef]
39. Ye, W.; Li, Y.; Wang, F. The improvement of the corrosion resistance of 309 stainless steel in the transpassive region by nano-crystallization. *Electrochim. Acta* **2009**, *54*, 1339–1349. [CrossRef]
40. Yanzhang, L.; Shaoyu, Q.; Xiaotao, Z.; Li, W.; Xinquan, H. A Study of Effect of Nitrogen Implantation on Corrosion Properties of Ti-Al-Zr Alloy. *Nucl. Phys. Rev.* **2006**, *23*, 202–206.
41. Xuewei, T.; Zhangzhong, W.; Zhixin, B.; Shixiao, K.; Qixiang, H. Research progress on surface modification technology of magnesium alloy ion implantation. *Mater. Rev.* **2014**, *28*, 112–115.
42. Heng, C.; Lin, L. Influence of residual stress on local corrosion behavior of metal materials. *Chin. J. Eng. Sci.* **2019**, *41*, 929–939.